Magnetic draping and cosmic-ray driven winds in galaxies

Christoph Pfrommer[1]

in collaboration with

Jonathan Dursi (magnetic draping)

Max Uhlig, Mahavir Sharma, Biman Nath, Torsten Enßlin, Volker Springel
(cosmic ray-driven winds)

[1] Heidelberg Institute for Theoretical Studies, Germany

Oct 30, 2012 / Astronomical Seminar Bochum

Outline

HITS

What is magnetic draping?

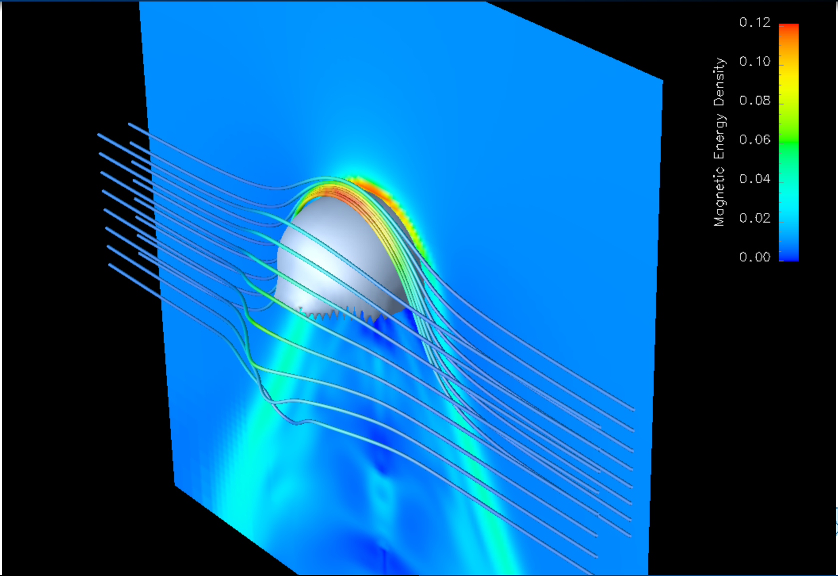

What is magnetic draping?

- Is magnetic draping (MD) similar to ram pressure compression?
  → no density enhancement for MD
  - analytical solution of MD for incompressible flow
  - ideal MHD simulations *(right)*
- Is magnetic flux still frozen into the plasma?
  yes, but plasma can also move along field lines while field lines get stuck at obstacle

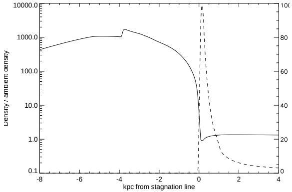

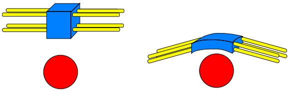

Draping of the interplanetary field over Venus

- Venus and Mars do not have a global magnetic field
- *Venus Express:* amplification of solar wind field by a factor ~ 6 at the side facing the Sun

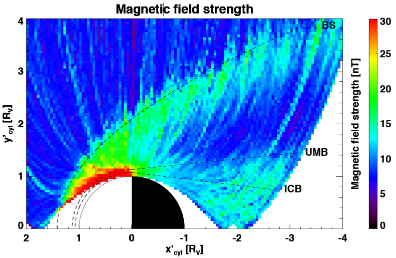

Guicking et al. (2010)

- draping of solar wind magnetic field around Venus/Mars leads to the formation of magnetic pile-up region and the magneto tail $\rightarrow$ enhanced magnetic field strength in the planets' wake

Magnetic draping in 2D

Sometimes,
2D just isn't
enough . . .

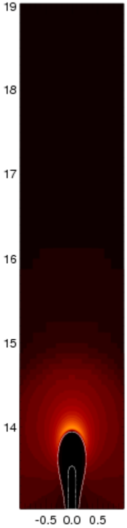

Streamlines in the rest frame of the galaxy

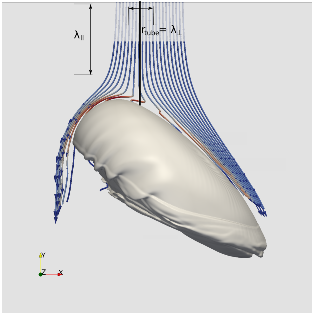

- analytic potential flow solution
  $\rightarrow$ critical impact parameter
  $p_{cr} = R/(2\mathcal{M}_A)$, $\mathcal{M}_A \simeq \mathcal{M}_s\sqrt{\beta} \sim 10$,
  R denotes the curvature radius
- only streamlines initially in a narrow tube of radius $p_{cr} \simeq R/20 \simeq 1$ kpc from the stagnation line become part of the magnetic draping layer (color coded) $\rightarrow$ constraints on λ_B
- the streamlines that do not intersect the tube get deflected away from the galaxy, become never part of the drape and eventually get accelerated (Bernoulli effect)
- note the kink feature in some draping-layer field lines due to back reaction as the solution changes from the hydrodynamic potential flow solution to that in the draped layer

Conditions for magnetic draping

- ambient plasma sufficiently ionized such that flux freezing condition applies
- super-Alfvénic motion of a cloud through a weakly magnetized plasma: $\mathcal{M}_A^2 = \beta\gamma\mathcal{M}^2/2 > 1$
- magnetic coherence across the "cylinder of influence":

$$\frac{\lambda_B}{R} \gtrsim \frac{1}{\mathcal{M}_A} \sim 0.1 \times \left(\frac{\beta}{100}\right)^{-1/2} \quad \text{for sonic motions,}$$

R denotes the curvature radius of the working surface at the stagnation line

Polarized synchrotron emission in a field spiral: M51

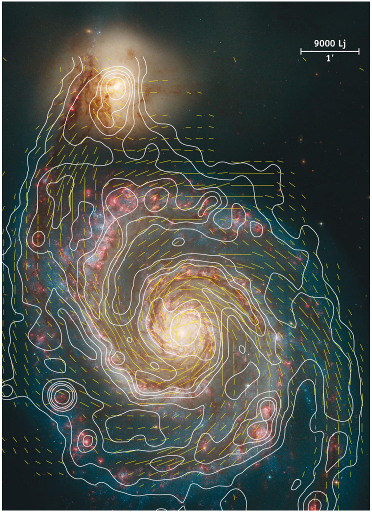

MPIfR Bonn and Hubble Heritage Team

- grand design ‘whirlpool galaxy’ (M51): optical star light superposed on radio contours
- polarized radio intensity follows the spiral pattern and is strongest in between the spiral arms
- the polarization ‘B-vectors’ are aligned with the spiral structure

Ram-pressure stripping of cluster spirals

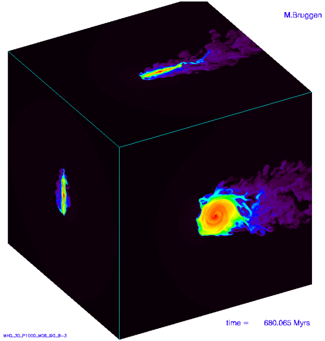

Brueggen (2008)

- 3D simulations show that the ram-pressure wind quickly strips the low-density gas in between spiral arms (Tonnesen & Bryan 2010)
- being flux-frozen into this dilute plasma, the large scale magnetic field will also be stripped

→ resulting radio emission should be unpolarized

Polarized synchrotron ridges in Virgo spirals

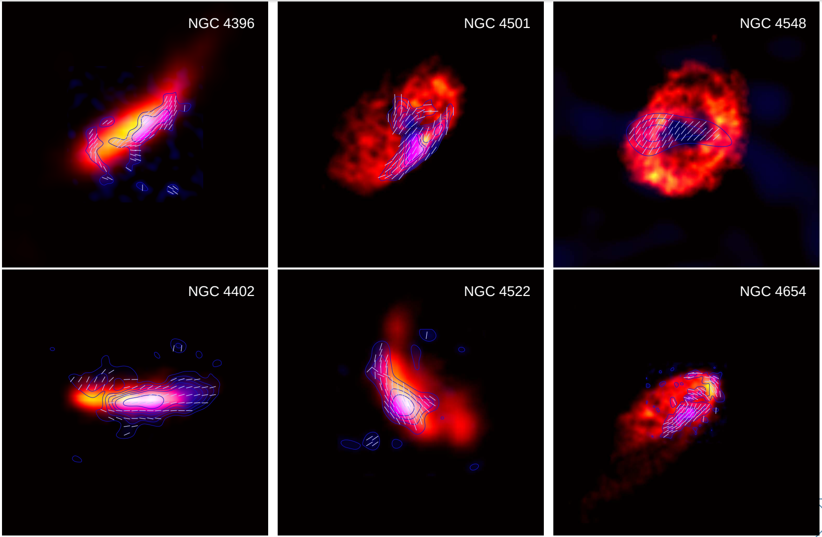

Vollmer et al. (2007): 6 cm PI (contours) + B-vectors; Chung et al. (2009): HI (red)

Observational evidence and model challenges

- asymmetric distributions of polarized intensity at the leading edge with extraplanar emission, sometimes also at the side
- coherent alignment of polarization vectors over ~ 30 kpc
- stars lead polarized emission, polarized emission leads gas
- HI gas only moderately enhanced (factor $\lesssim 2$), localized 'HI hot spot' smaller than the polarized emission region: $n_{\text{compr}} \simeq n_{\text{icm}}\, v_{\text{gal}}^2 / c_{\text{ism}}^2 \simeq 1\,\text{cm}^{-3} \simeq \langle n_{\text{ism}} \rangle$
- flat radio spectral index (similar to the Milky Way) that steepens towards the edges of the polarized ridge
- no or weak Kelvin-Helmholtz instabilities at interface detectable

$\rightarrow$ previous models that use ram-pressure compressed galactic magnetic fields fail to explain most of these points!

Observational evidence and model challenges

- asymmetric distributions of polarized intensity at the leading edge with extraplanar emission, sometimes also at the side
- coherent alignment of polarization vectors over $\sim$ 30 kpc
- stars lead polarized emission, polarized emission leads gas
- HI gas only moderately enhanced (factor $\lesssim 2$), localized 'HI hot spot' smaller than the polarized emission region: $n_\mathrm{compr} \simeq n_\mathrm{icm}\, v_\mathrm{gal}^2 / c_\mathrm{ism}^2 \simeq 1\,\mathrm{cm}^{-3} \simeq \langle n_\mathrm{ism} \rangle$
- flat radio spectral index (similar to the Milky Way) that steepens towards the edges of the polarized ridge
- no or weak Kelvin-Helmholtz instabilities at interface detectable

$\rightarrow$ need to consider the full MHD of the interaction spiral galaxy and magnetized ICM !

Magnetic draping around a spiral galaxy

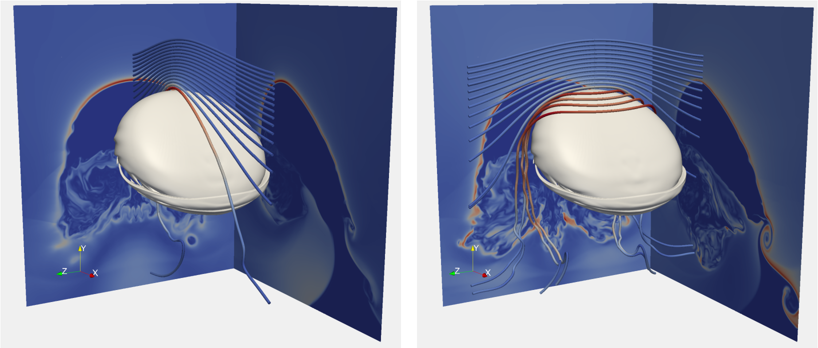

Athena simulations of spiral galaxies interacting with a uniform cluster magnetic field; there is a sheath of strong field draped around the leading edge (shown in red)

C.P. & Dursi (2010)

HITS

Magnetic draping around a spiral galaxy – physics

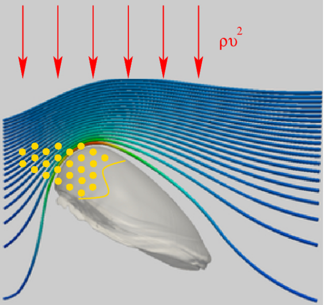

- the galactic ISM is pushed back by the ram pressure wind $\sim \rho v^2$
- the stars are largely unaffected and lead the gas
- the draping sheath is formed at the contact of galaxy/cluster wind
- as stars become SN, their remnants accelerate CRes that populate the field lines in the draping layer

- CRes are transported diffusively (along field lines) and advectively as field lines slip over the galaxy
- CRes emit radio synchrotron radiation in the draped region, tracing out the field lines there $\rightarrow$ coherent polarized emission at the galaxies' leading edges

Modeling the electron population

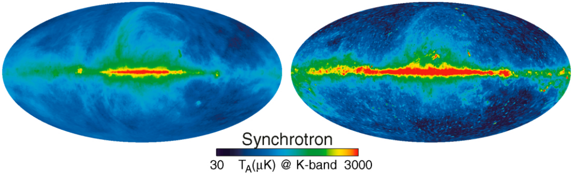

- typical SN rates imply a homogeneous CRe distribution (WMAP)
- FIR-radio correlation of Virgo spirals show comparable values to the solar circle → take CRe distribution of our Galaxy:

$$n_{\rm cre} = C_0\, e^{-(R-R_\odot)/h_R}\, e^{-|z|/h_z}$$

with normalization $C_0 \simeq 10^{-4}\,\text{cm}^{-3}$,
scale heights $h_R \simeq 8\,\text{kpc}$ and $h_z \simeq 1\,\text{kpc}$ at Solar position

- truncate at contact of ISM-ICM, attach exp. CRe distribution ⊥ to contact surface with $h_\perp \simeq 150$ pc (max. radius of Sedov phase)

Magnetic draping and polarized synchrotron emission

Synchrotron B-vectors reflect the upstream orientation of cluster magnetic fields

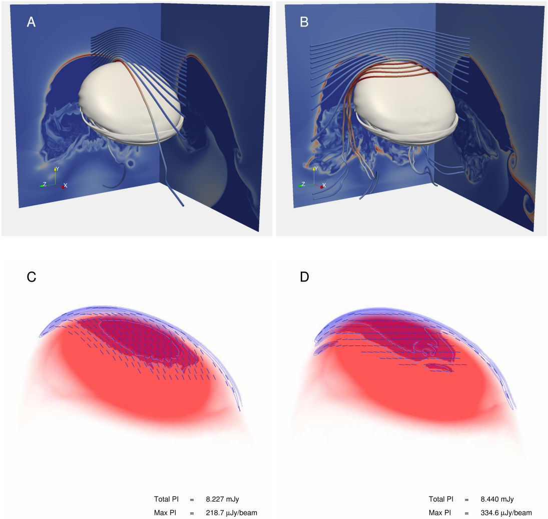

Simulated polarized synchrotron emission

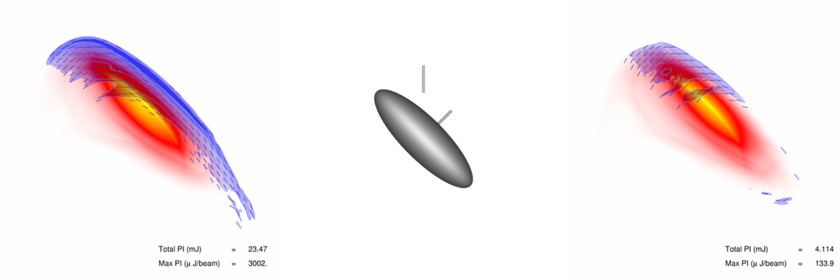

Movie of the simulated polarized synchrotron radiation viewed from various angles and with two field orientations.

Magnetic draping of a helical B-field

(Non-)observation of polarization twist constrains magnetic coherence length

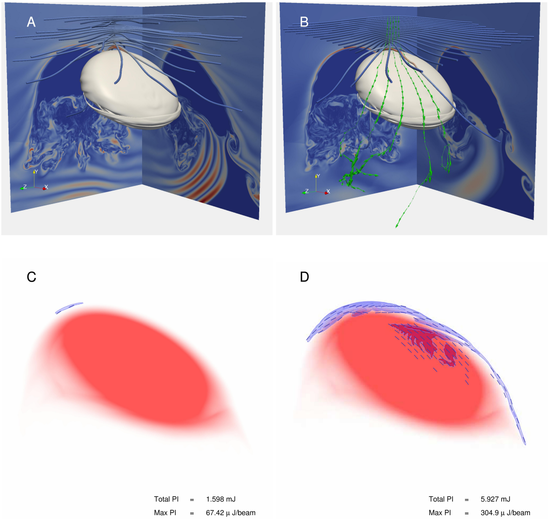

Varying galaxy inclination and magnetic tilt

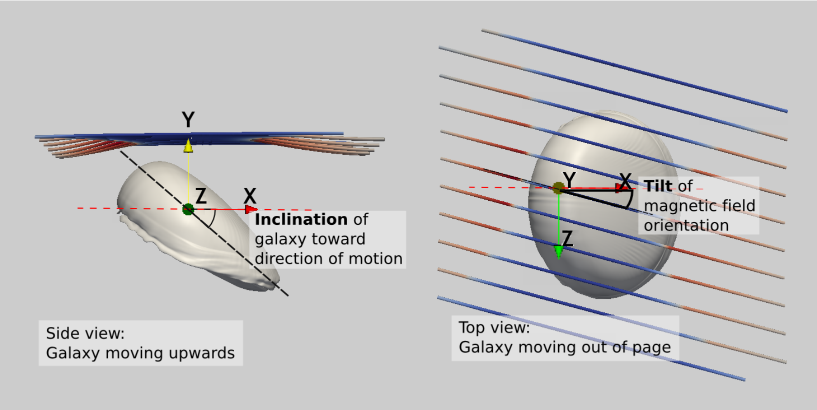

Observations versus simulations

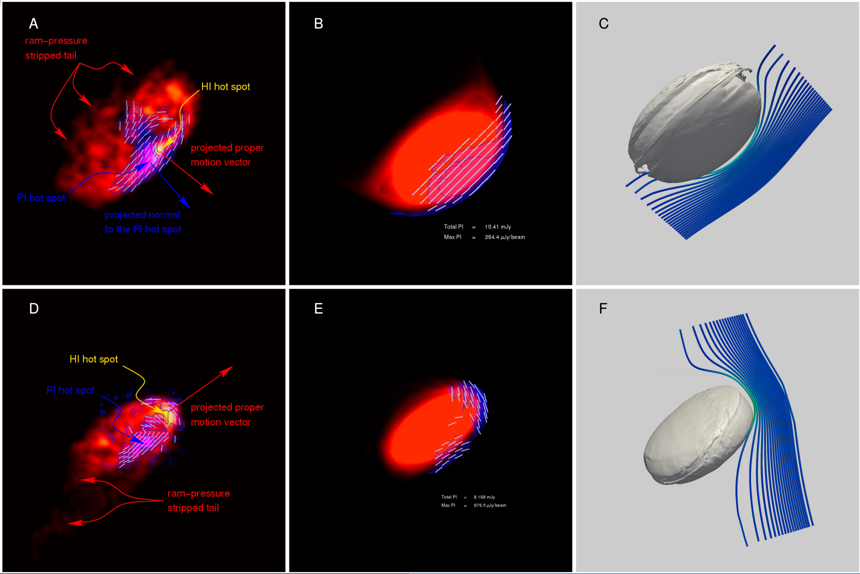

Mapping out the magnetic field in Virgo

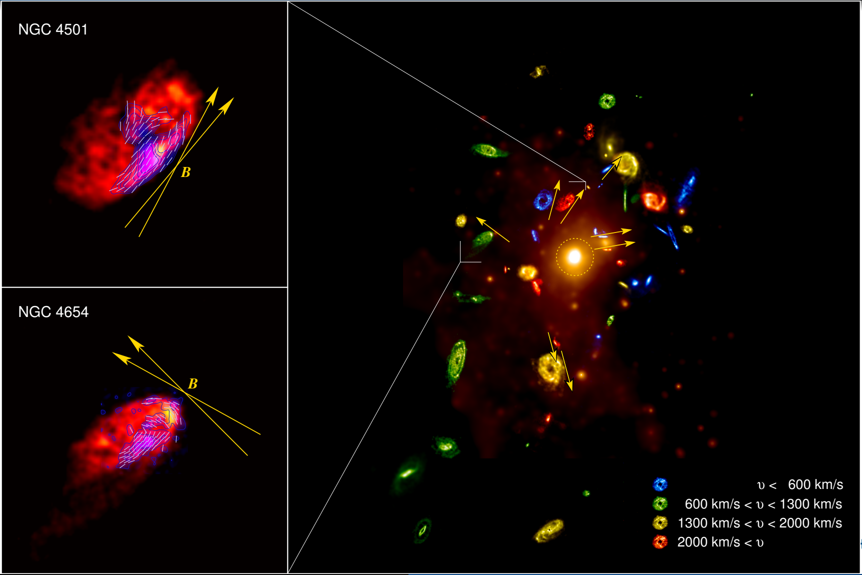

HITS

Discussion of radial field geometry

- the alignment of the field in the plane of the sky is significantly more radial than expected from random chance; considering the sum of deviations from radial alignment gives a chance coincidence of less than 1.7% ($\sim 2.2\,\sigma$)
- for the three nearby galaxy pairs in the data set, all have very similar field orientations

$\rightarrow$ Which effect causes this field geometry?

Magneto-thermal instability? (Parrish+2007, C.P.+2010)
Radial infall? (Ruszkowski+2010)

Conclusions on magnetic draping around galaxies

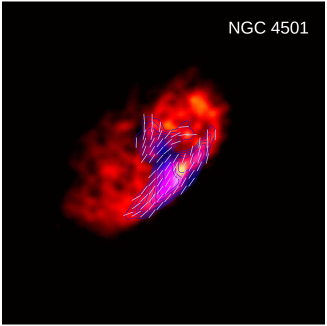

- draping of cluster magnetic fields naturally explains polarization ridges at Virgo spirals

Conclusions on magnetic draping around galaxies

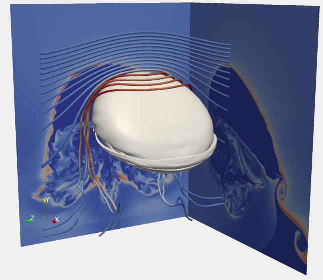

- draping of cluster magnetic fields naturally explains polarization ridges at Virgo spirals
- this represents a new tool for measuring the in situ 3D orientation and coherence scale of cluster magnetic fields

Conclusions on magnetic draping around galaxies

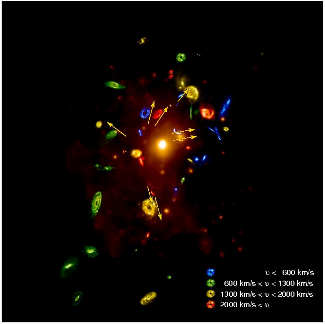

- draping of cluster magnetic fields naturally explains polarization ridges at Virgo spirals
- this represents a new tool for measuring the in situ 3D orientation and coherence scale of cluster magnetic fields
- application to the Virgo cluster shows that the magnetic field is preferentially aligned radially

Conclusions on magnetic draping around galaxies

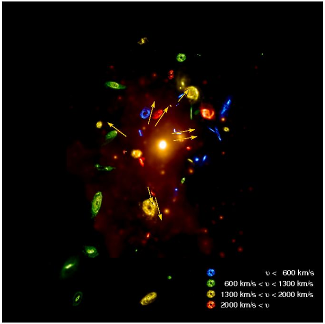

- draping of cluster magnetic fields naturally explains polarization ridges at Virgo spirals
- this represents a new tool for measuring the in situ 3D orientation and coherence scale of cluster magnetic fields
- application to the Virgo cluster shows that the magnetic field is preferentially aligned radially

- this finding implies efficient thermal conduction across clusters → important for thermal cluster history/cluster cosmology
- outlook: draping on cosmological galaxies, follow CR electron transport, . . .

Galactic super wind in M82

Galactic wind in the Milky Way?

Diffuse X-ray emission in our galaxy

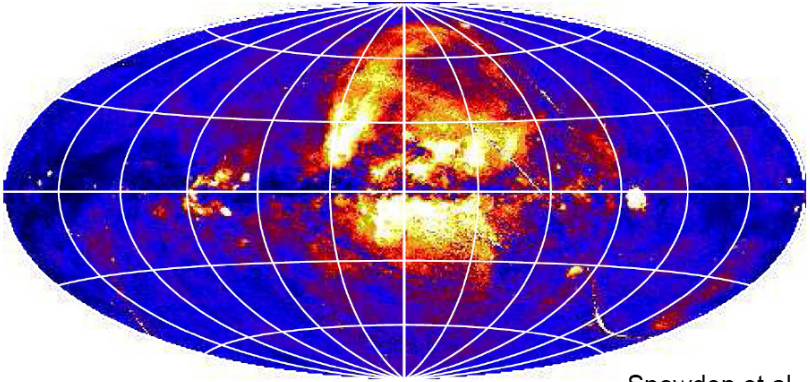

Snowden et al., 2007

Galactic wind in the Milky Way?

Fermi gamma-ray bubbles

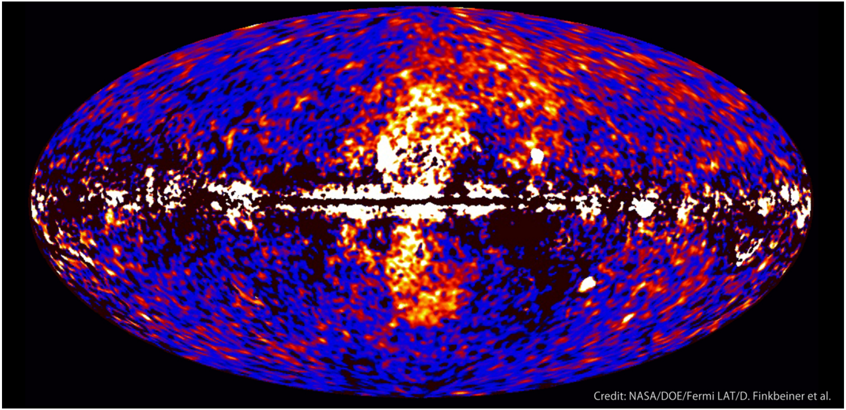

Galactic wind trivia

Winds . . .

- . . . may explain mismatch between luminosity function and halo mass function on small scales
- . . . may enrich the intergalactic medium (IGM) with metals and magnetic fields
- . . . influence energy budget of IGM

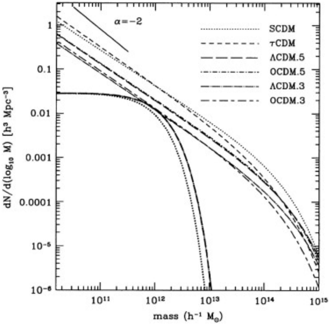

Somerville+1999

How to drive a wind?

- standard picture: wind driven by thermal pressure
- energy sources for winds: supernovae, AGN
- problem with the standard picture: fast radiative cooling
- alternative channels:
    - radiation pressure on dust grains
    - cosmic rays (CRs, relativistic protons with $\gamma_{\rm ad} = 4/3$)

Radio halos in edge-on disk galaxies

CRs and magnetic fields exist at the disk-halo interface → wind launching site?

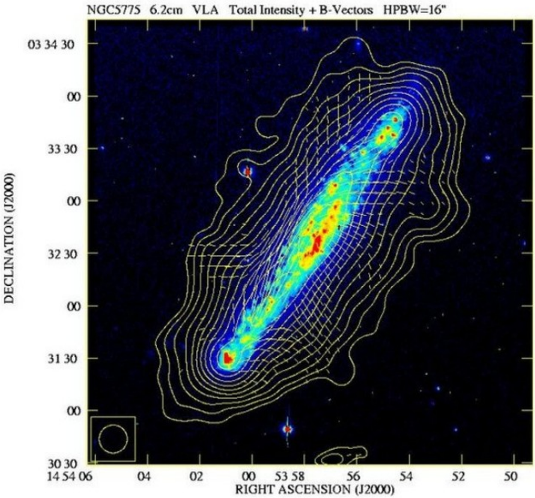

Tüllmann+2000

Cosmic ray-driven winds

- several reasons why CRs are important for wind formation:
  - CR pressure drops less quickly than thermal pressure ($P \propto \rho^\gamma$)
  - CRs cool less efficiently than thermal gas
  - most CR energy loss goes into thermal pressure
- analytical models: CR can aid in driving winds
  (Ipavich 1975, Breitschwerdt+1991, Socrates+2008, Everett+2008/2010, Samui2010)
- up to now, no 3D hydrodynamical simulations that study CR driven winds!

Uhlig, C.P., Sharma, Nath, Enßlin, Springel, *MNRAS* **423**, 2374 (2012)
Galactic winds driven by cosmic-ray streaming

Interstellar medium (ISM) simulations – flowchart

ISM observables:

Physical processes in the ISM:

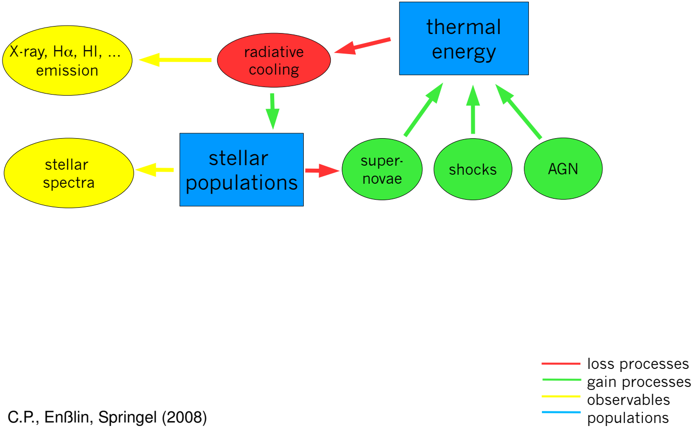

C.P., Enßlin, Springel (2008)

ISM simulations with cosmic ray physics

ISM observables: Physical processes in the ISM:

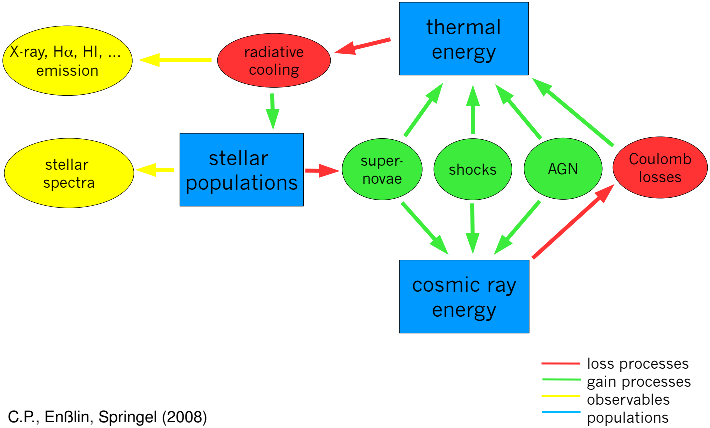

C.P., Enßlin, Springel (2008)

ISM simulations with extended cosmic ray physics

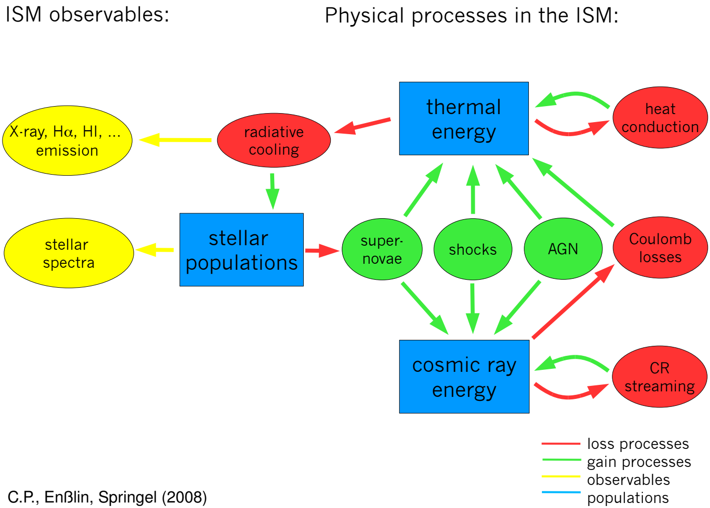

C.P., Enßlin, Springel (2008)

ISM simulations with extended cosmic ray physics

ISM observables: Physical processes in the ISM:

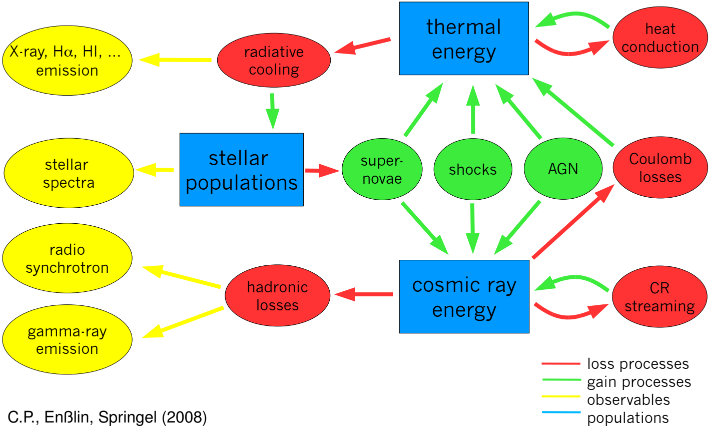

C.P., Enßlin, Springel (2008)

Interactions of CRs and magnetic fields

- CRs scatter on magnetic fields → isotropization of CR momenta
- **CR streaming instability:** Kulsrud & Pearce 1969
  - if $v_{\rm cr} > v_{\rm waves}$ with respect to the gas, CR excite Alfvén waves
  - scattering off this wave field limits the CRs' bulk speed $\ll c$
  - wave damping: transfer of CR energy and momentum to the thermal gas

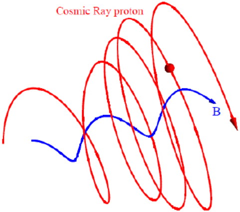

→ **CRs exert a pressure on the thermal gas by means of scattering off Alfvén waves**

CR streaming (1)

- total CR velocity $\boldsymbol{v}_{\mathrm{cr}} = \boldsymbol{v}_{\mathrm{gas}} + \boldsymbol{v}_{\mathrm{st}}$
- CRs stream down their own pressure gradient relative to the gas:

$$\boldsymbol{v}_{\mathrm{st}} = -\lambda\, c_{\mathrm{s}}\, \frac{\nabla P_{\mathrm{cr}}}{|\nabla P_{\mathrm{cr}}|},$$

- CR transport equation → evolution equation for CR number and energy density:

$$\begin{aligned}
\frac{\partial n_{\mathrm{cr}}}{\partial t} &= -\nabla \cdot \left[\left(\boldsymbol{v}_{\mathrm{gas}} + \boldsymbol{v}_{\mathrm{st}}\right) n_{\mathrm{cr}}\right] \\
\frac{\partial \varepsilon_{\mathrm{cr}}}{\partial t} &= \left(\boldsymbol{v}_{\mathrm{gas}} + \boldsymbol{v}_{\mathrm{st}}\right) \cdot \nabla P_{\mathrm{cr}} - \nabla \cdot \left[\left(\boldsymbol{v}_{\mathrm{gas}} + \boldsymbol{v}_{\mathrm{st}}\right)\left(\varepsilon_{\mathrm{cr}} + P_{\mathrm{cr}}\right)\right]
\end{aligned}$$

CR streaming (2)

- Lagrangian time derivative

$$\frac{\mathrm{d}}{\mathrm{d}t} = \frac{\partial}{\partial t} + \boldsymbol{v}_{\mathrm{gas}} \cdot \nabla$$

- specific CR energy, $\tilde{\varepsilon}_{\mathrm{cr}}$, and CR particle number, $\tilde{n}_{\mathrm{cr}}$,

$$\varepsilon_{\mathrm{cr}} = \tilde{\varepsilon}_{\mathrm{cr}}\rho \qquad \text{and} \qquad n_{\mathrm{cr}} = \tilde{n}_{\mathrm{cr}}\rho$$

- CR evolution equations:

$$\rho\frac{\mathrm{d}\tilde{n}_{\mathrm{cr}}}{\mathrm{d}t} = -\nabla \cdot [\boldsymbol{v}_{\mathrm{st}}\,\rho\,\tilde{n}_{\mathrm{cr}}]$$

$$\rho\frac{\mathrm{d}\tilde{\varepsilon}_{\mathrm{cr}}}{\mathrm{d}t} = \underbrace{\boldsymbol{v}_{\mathrm{st}} \cdot \nabla P_{\mathrm{cr}}}_{\substack{\text{energy loss term}\\ \text{(wave damping)}}} - \underbrace{P_{\mathrm{cr}}\nabla \cdot \boldsymbol{v}_{\mathrm{gas}}}_{\substack{\text{adiabatic changes}\\ \text{due to converging/}\\ \text{diverging gas flow}}} - \underbrace{\nabla \cdot [\boldsymbol{v}_{\mathrm{st}}\,(\rho\tilde{\varepsilon}_{\mathrm{cr}} + P_{\mathrm{cr}})]}_{\substack{\text{energy change due to}\\ \text{CR streaming in/out}\\ \text{of a volume element}}}$$

Test: Gadget-2 versus 1-d grid solver

Evolution of the specific CR energy due to streaming in a medium at rest

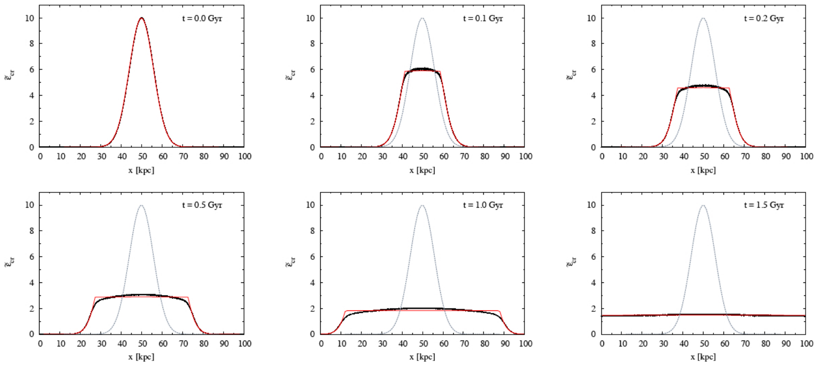

Uhlig+2012

Simulation setup

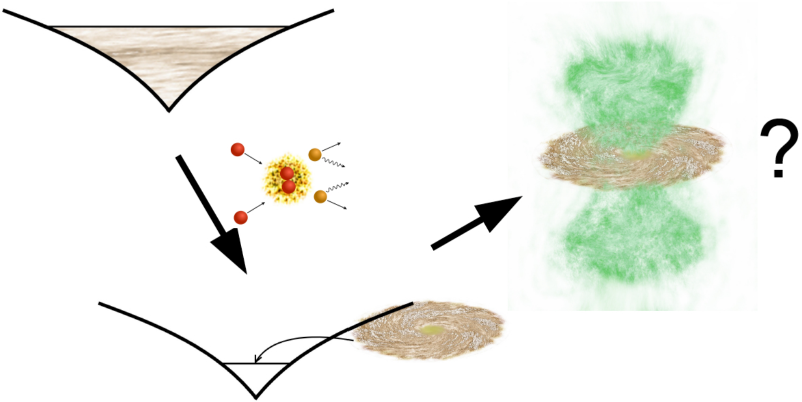

CR streaming drives winds

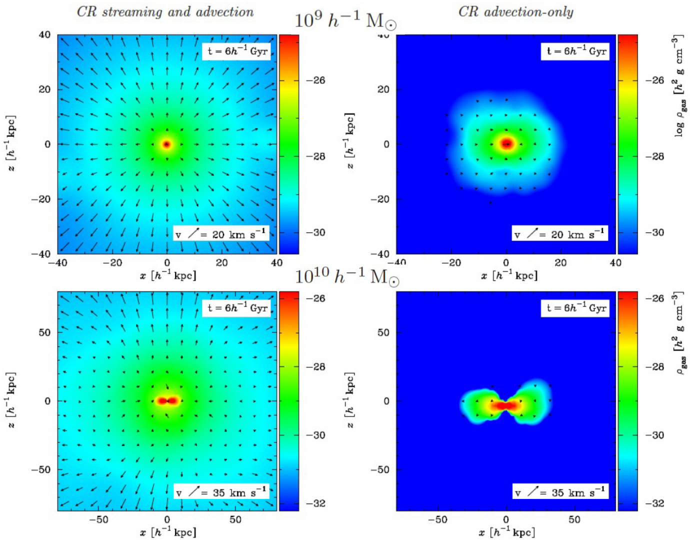

Wind velocity profile along the symmetry axis

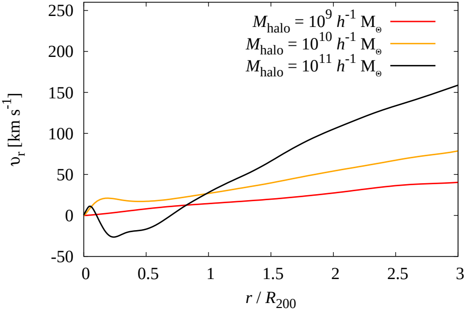

- $10^9 - 10^{10}\,M_\odot$: accelerating wind due to a continuous CR momentum and energy deposition during the ascent of the wind in the gravitational potential
- $10^{11}\,M_\odot$: wind stalls in halo and falls back onto the disk $\rightarrow$ fountain flow

CR-to-thermal pressure in edge-on slice

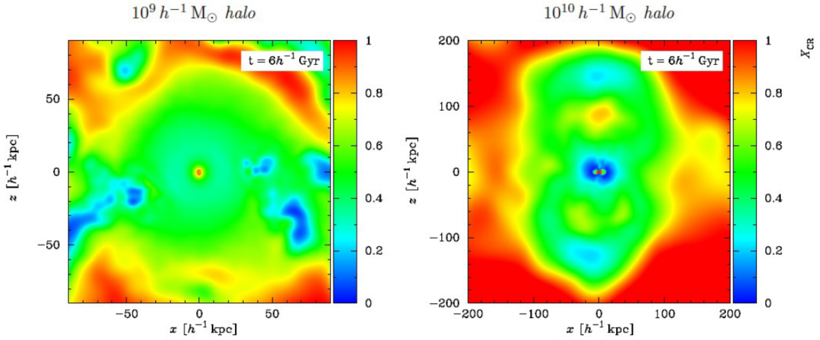

- $X_{\mathrm{cr}} = P_{\mathrm{cr}}/P < 50\%$ in vicinity of center because of loss processes that effectively transfer CR into thermal energy
- X_{cr} becomes dominant at larger heights due to the softer adiabatic index of CRs

Gas mass loss within the virial radius

different scenarios:

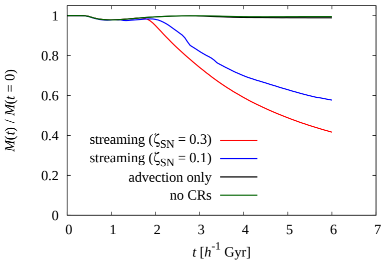

different galaxy masses:

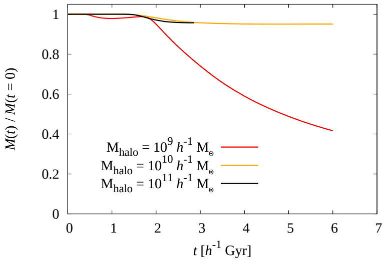

- after initial phase ($\sim$ 2.5 Gyr), only winds driven by CR streaming overcome the ram pressure of infalling gas and expel gas from the halo
- mass loss rate increases with CR injection efficiency $\zeta_{\rm SN}$ *(left)* and towards smaller galaxy masses *(right)*

HITS

Mass loss and star formation rates

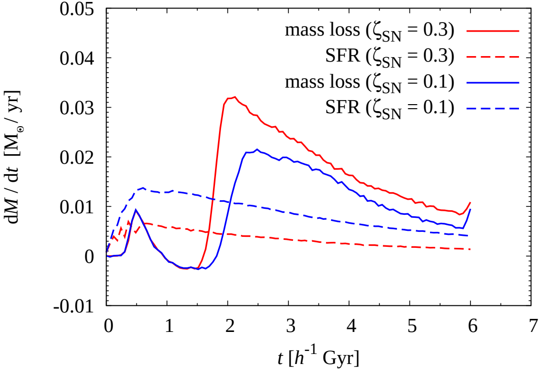

- time lag between onset of star formation and associated supernovae (that inject CRs) and mass loss rate (from R_{200})

$$10^9\, h^{-1} \mathrm{M}_\odot : \qquad \tau_{\rm lag} = \frac{R_{200}}{v_{\rm esc}} \simeq \frac{20\,\mathrm{kpc}}{20\,\mathrm{km\,s}^{-1}} \simeq 1\,\mathrm{Gyr}$$

Mass loss and star formation histories

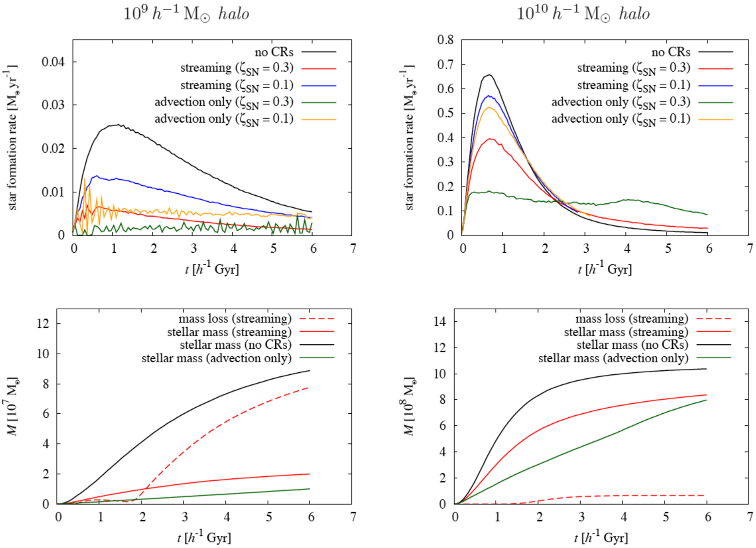

Heating of the halo gas by wave damping

$10^{10}\ h^{-1} M_\odot$:

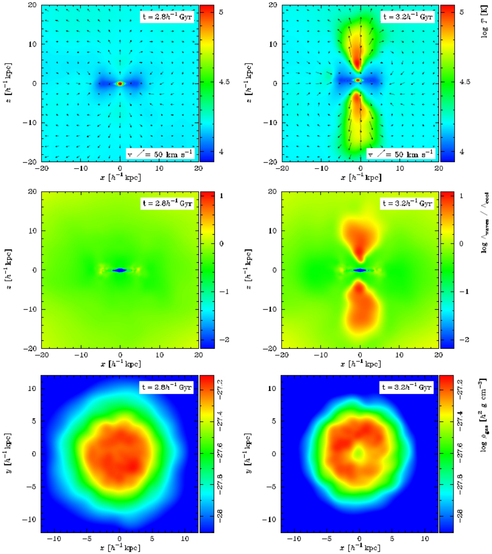

Temperature structure

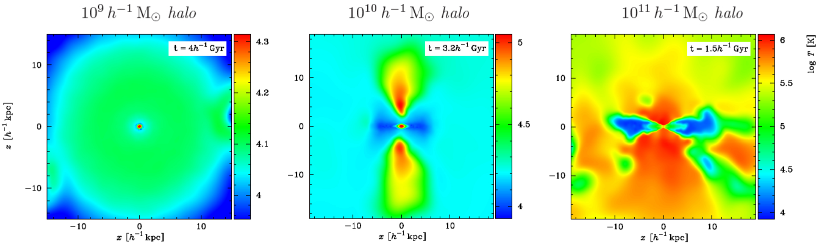

- halo temperatures scale as $kT \propto v_{\mathrm{wind}}^2 \sim v_{\mathrm{esc}}^2$
- $10^9 \rightarrow 10^{10}\,M_\odot$: transition of isotropic to bi-conical wind; in these cones, CR wave heating overcomes radiative cooling
- $10^{10} \rightarrow 10^{11}\,M_\odot$: broadening of hot temperature structure due to inability of CR streaming to drive a sustained wind; instead, fountain flows drive turbulence, thereby heating larger regions

Gas temperature: simulation ($10^{10}\,M_\odot$) vs. observation

t = 4.9 Gyr, streaming

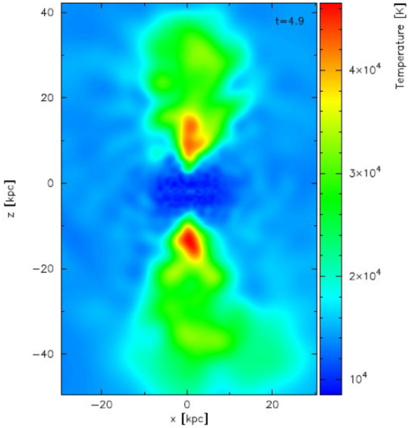

M82

HITS

Hα emission (10^{10} M$_\odot$)

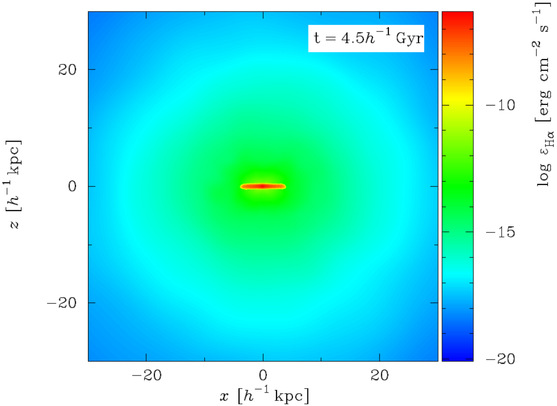

- diffuse Hα emission by ionized gas, entrained in the wind
- no conical, filamentary structure as in M82: numerics, missing physics, . . . ?

CR-driven winds: analytics versus simulations

Wind speeds and mass loading factors

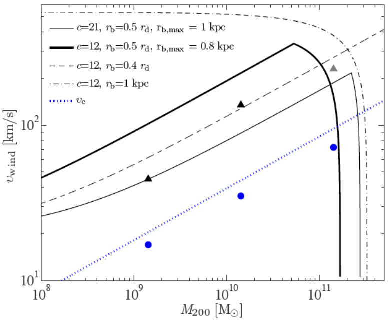

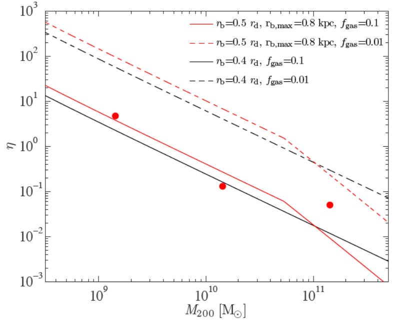

- winds speeds increase with galaxy mass as $v_{\rm wind} \propto v_{\rm circ} \propto M_{200}^{1/3}$ until they cutoff around 10^{11} M$_\odot$ due to a fixed wind base height (set by radiative physics)
- mass loading factor $\eta = \dot{M}/\mathrm{SFR}$ decreases with galaxy mass

Comparing different wind launching mechanisms

Galactic winds driven by CR streaming, ram and radiation pressure

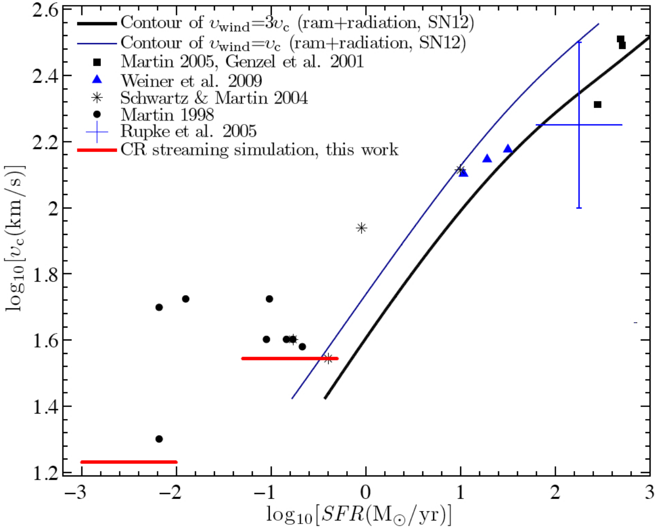

Conclusions on cosmic-ray driven winds in galaxies

- galactic winds are naturally explained by CR streaming (energy source, known plasma physics, observed scaling relations)
- CR streaming heating can explain observed hot wind regions above disks
- substantial mass losses of low mass galaxies
  $\rightarrow$ opportunity for understanding the physics at the faint end of galaxy luminosity function

outlook: MHD simulations, better understanding of plasma physics, cosmological settings, . . .

Literature for the talk

Magnetic draping:

- Pfrommer & Dursi, *Detecting the orientation of magnetic fields in galaxy clusters*, Nature Phys., 6, 5206, 2010.
- Dursi & Pfrommer, *Draping of cluster magnetic fields over bullets and bubbles – morphology and dynamic effects*, ApJ, 677, 993, 2008.

CR-driven winds in galaxies:

- Uhlig, Pfrommer, Sharma, Nath, Enßlin, Springel, *Galactic winds driven by cosmic-ray streaming*, MNRAS, 423, 2374, 2012.

Additional slides

Resolution study

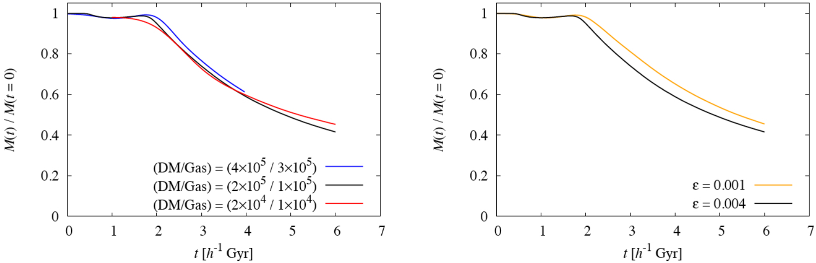

- our results winds driven by CR streaming are converged with respect to particle resolution *(left)* and time step of the explicit streaming solver *(right)*

Magnetic coherence scale estimate by radio ridges

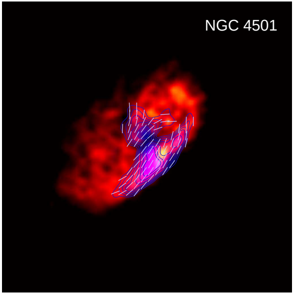

- observed polarised draping emission $\rightarrow$ field coherence length λ_B is at least galaxy-sized
- if $\lambda_B \sim 2R_{\rm gal}$, then the change of orientation of field vectors imprint as a change of the polarisation vectors along the vertical direction of the ridge showing a 'polarisation-twist'

- the reduced speed of the boundary flow means that a small $L_{\rm drape}$ corresponds to a larger length scale of the unperturbed magnetic field ahead of the galaxy NGC 4501

$$L_{\rm coh} \simeq \eta L_{\rm drape} v_{\rm gal}/v_{\rm drape} = \eta \tau_{\rm syn} v_{\rm gal} > 100\,\rm kpc,$$

with $\tau_{\rm syn} \simeq 5 \times 10^7$ yr, $v_{\rm gal} \simeq 1000\,\rm km/s$, and a geometric factor $\eta \simeq 2$

Biases in inferring the field orientation

- uncertainties in estimating the 3D velocity: v_r, ram-pressure stripped gas visible in HI morphology $\rightarrow \hat{\boldsymbol{v}}_\mathrm{t}$
- *direction-of-motion asymmetry:* magnetic field components in the direction of motion bias the location of $B_{\mathrm{max,\ drape}}$ (figure to the right): draping is absent if $\boldsymbol{B} \parallel \boldsymbol{v}_\mathrm{gal}$

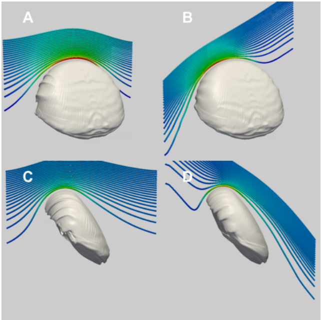

- *geometric bias:* polarized synchrotron emission only sensitive to traverse magnetic field B_t ($\perp$ to LOS) $\rightarrow$ maximum polarised intensity may bias the location of $B_{\mathrm{max,\ drape}}$ towards the location in the drape with large B_t

Magnetic draping with LOFAR

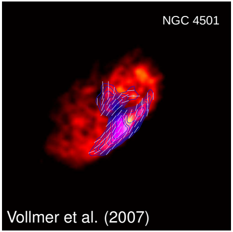

- NGC 4501: 5 GHz polarized intensity
- lower frequency
  → longer electron cooling time
  → larger magnetic drape!
- length scale of draping sheath:

$$\gamma = \left(\frac{2\pi\nu_{\rm syn} m_{\rm e} c}{3eB}\right)^{1/2} \simeq 10^4 \left(\frac{\nu_{\rm syn}}{5\,\rm GHz}\right)^{1/2} \left(\frac{B}{7\,\mu\rm G}\right)^{-1/2},$$

$$\tau_{\rm syn} = \frac{6\pi m_{\rm e} c}{\sigma_{\rm T} B^2 \gamma} \simeq 50\,{\rm Myr} \left(\frac{\nu_{\rm syn}}{5\,\rm GHz}\right)^{-1/2} \left(\frac{B}{7\,\mu\rm G}\right)^{-3/2},$$

$$L_{\rm drape} = \eta v_{\rm drape} \tau_{\rm syn} \simeq 10\,{\rm kpc} \left(\frac{\nu_{\rm syn}}{5\,\rm GHz}\right)^{-1/2} \simeq 60\,{\rm kpc} \left(\frac{\nu_{\rm syn}}{150\,\rm MHz}\right)^{-1/2},$$

with velocity in draping layer $v_{\rm drape} \simeq 100\,{\rm km\,s}^{-1}$ and a geometric factor $\eta \simeq 2$.

Magneto-thermal instability: the idea

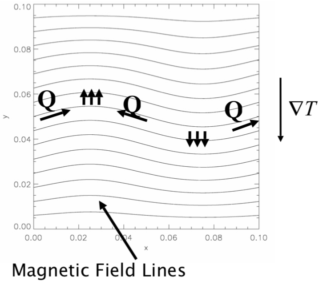

Figure from I. Parrish

Convective stability in a gravitational field:

- Classical Schwarzschild criterion: $\frac{\mathrm{d}S}{\mathrm{d}z} > 0$
- long MFP, Balbus criterion: $\frac{\mathrm{d}T}{\mathrm{d}z} > 0$
- new instability causes field lines to reorient radially $\rightarrow$ efficient thermal conduction radially (close to Spitzer)

The non-linear behavior of the MTI (Parrish & Stone 2007).

- Adiabatic boundary conditions for $T(r)$: the instability can exhaust the source of free energy $\rightarrow$ isothermal profile
- Fixed boundary conditions for $T(r)$: field lines stay preferentially radially aligned (35 deg mean deviation from radial)

Gravitational shock wave heating

Observed temperature profile in clusters is decreasing outwards
→ heat also flows outwards along the radial magnetic field.
How is the temperature profile maintained? → gravitational heating

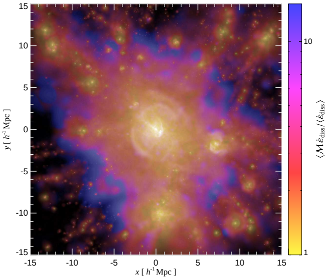

shock strengths weighted by dissipated energy

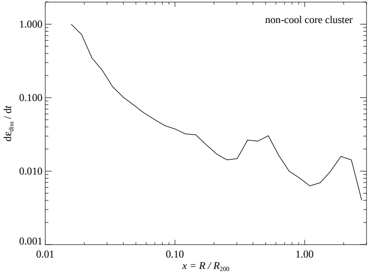

energy flux through shock surface
$\dot{E}_{\rm diss}/R^2 \sim \rho v^3$
→ increase towards the center

HITS